JGR

RESEARCH ARTICLE

Key Points:
- Published diffusion models produced soil efflux underestimations from 55% to 361%
- Determining in situ diffusion estimates using conservative tracer injections did not produce favorable results
- Calibrating a gas transfer model using automated chambers produced accurate long-term soil effluxes

Improving the accuracy of the gradient method for determining soil carbon dioxide efflux

Enrique P. Sánchez-Cañete[1,2] (iD), Russell L. Scott[3] (iD), Joost van Haren[1,4] (iD), and Greg A. Barron-Gafford[1,5] (iD)

[1]B2 Earthscience, Biosphere 2, University of Arizona, Tucson, Arizona, USA, [2]Centro Andaluz de Medio Ambiente (IISTA-CEAMA), Granada, Spain, [3]Southwest Watershed Research Center, USDA-ARS, Tucson, Arizona, USA, [4]Honors College, University of Arizona, Tucson, Arizona, USA, [5]School of Geography and Development, University of Arizona, Tucson, Arizona, USA

Abstract Soil CO_2 efflux (F_{soil}) represents a significant source of ecosystem CO_2 emissions that is rarely quantified with high-temporal-resolution data in carbon flux studies. F_{soil} estimates can be obtained by the low-cost gradient method (GM), but the utility of the method is hindered by uncertainties in the application of published models for the diffusion coefficient. Therefore, to address and resolve these uncertainties, we compared F_{soil} measured by 2 soil CO_2 efflux chambers and F_{soil} estimated by 16 gas transport models using the GM across 1 year. We used 14 published empirical gas diffusion models and 2 in situ models: (1) a gas transfer model called "Chamber model" obtained using a calibration between the chamber and the gradient method and (2) a diffusion model called "SF_6 model" obtained through an interwell conservative tracer experiment. Most of the published models using the GM underestimated cumulative annual F_{soil} by 55% to 361%, while the Chamber model closely approximated cumulative F_{soil} (0.6% error). Surprisingly, the SF_6 model combined with the GM underestimated F_{soil} by 32%. Differences between in situ models could stem from the Chamber model implicitly accounting for production of soil CO_2, while the conservative tracer model does not. Therefore, we recommend using the GM only after calibration with chamber measurements to generate reliable long-term ecosystem F_{soil} measurements. Accurate estimates of F_{soil} will improve our understanding of soil respiration's contribution to ecosystem fluxes.

1. Introduction

Soil CO_2 efflux (F_{soil}) represents a significant source of terrestrial CO_2 emissions [*Raich and Schlesinger*, 1992], and our ability to accurately represent F_{soil} and soil carbon stocks is key for accurately predicting carbon-climate feedback [*Todd-Brown et al.*, 2012]. Because of their large global magnitude, even small changes in soil CO_2 effluxes (F_{soil}) directly affect the atmospheric CO_2 content [*Raich and Schlesinger*, 1992], leaving F_{soil} as one of the most poorly constrained components of the terrestrial carbon cycle [*Bond-Lamberty and Thomson*, 2010]. Much of this uncertainty in this dominant flux stems from the fact that models of F_{soil} are not well estimated, as both positive and negative feedback between belowground carbon pools and effluxes, and temperature sensitivity in future climate scenarios largely ignored [*Davidson and Janssens*, 2006]. Most often, F_{soil} is measured using manual or automated soil chambers [*Pumpanen et al.*, 2004]. Manual chamber measurements have been frequently used due to their ease in deployment, but the sampling frequency is often low, normally weekly, monthly, or seasonally and often only during the daytime in fair weather conditions [*Janssens et al.*, 2001a]. Automated chamber systems are more desirable as they allow for near-continuous (every 30 min or hourly) measurements of F_{soil} over longer periods of time [*Drewitt et al.*, 2002; *Hamerlynck et al.*, 2013; *Oishi et al.*, 2013], but deployment of these systems is limited due to their higher costs. Continuous estimation of F_{soil} can also be obtained by application of the gradient method (GM), where the soil CO_2 molar fraction is measured at different depths [*Tang et al.*, 2003; *Maier and Schack-Kirchner*, 2014; *Sanchez-Canete and Kowalski*, 2014]. This technique has been readily adopted due to the development of new low-cost and low-power CO_2 sensors. However, despite their widespread use, the utility of the GM is hindered by uncertainties associated with the application of ex situ published models of the soil diffusion coefficient (D_s [*Werner et al.*, 2004; *Allaire et al.*, 2008]).

D_s is the only modeled parameter in the gradient method, yet its estimation is highly uncertain. Most researchers have applied a D_s model from the literature to estimate the F_{soil} [*Pumpanen et al.*, 2003; *Tang et al.*, 2003; *Davidson et al.*, 2006; *Rains et al.*, 2016], but a few have determined D_s for their soils of interest, either in the

laboratory using field samples [*Jassal et al.*, 2005; *Maier et al.*, 2010; *Schack-Kirchner et al.*, 2011] or in situ [*Roland et al.*, 2015]. Recent studies demonstrate the enormous uncertainty in computed F_{soil} associated with different D_s models [*Pingintha et al.*, 2010; *Roland et al.*, 2015], suggesting that in situ estimation of D_s is necessary. In situ measurements of the soil diffusion coefficient can be determined through two different techniques [*Werner et al.*, 2004]. First, the most common technique uses a tracer gas that is either a natural tracer such as radon [*Davidson and Trumbore*, 1995; *Uchida et al.*, 1997; *Ota and Yamazawa*, 2010] or a biologically inactive gas such as sulfur hexafluoride (SF_6) injected directly into the soil [*Ball et al.*, 1994; *Johnson et al.*, 1998; *Shcherbak and Robertson*, 2014]. The other, less common, technique uses the GM to determine the apparent diffusion coefficient (D_{app}), also called the gas transfer coefficient (k_s), in situ, by measuring the CO_2 molar fraction at two depths and F_{soil} from a chamber [*Roland et al.*, 2015]. This k_s is a more appropriate description of the parameter than a diffusion coefficient because k_s implicitly accounts for diffusive and nondiffusive transport as well as the production or consumption processes that can occur in the between-gradient soil layer.

The main goal of this paper was to obtain accurate long-term F_{soil} estimates based on the gradient method (GM). For that, we compare the 2 in situ methods for determining D_s and k_s and quantify the differences among the resultant D_s and k_s models based on porosity and soil water content with 14 D_s published models. Based on these models we obtained the F_{soil} by the GM, which we compared to F_{soil} measurements from two automated soil CO_2 chambers over a 1 year period. We address the following questions: (1) Given the large interests in understanding soil CO_2 dynamics, but the significant uncertainties created by the range of methodologies, how can we best estimate cumulative F_{soil}? (i.e., what are the best practices for the accurate measurement of long-term soil efflux?) (2) Can we use limited chamber efflux measurements, such as when the field conditions are highly variable (e.g., after a precipitation pulse), in place of a complete year of chamber effluxes to obtain an accurate k_s model that accurately estimates F_{soil}? Finally, to respond to other studies that found poor agreements between subdaily F_{soil} measurements using soil chambers and estimates using the GM [*Goffin et al.*, 2015; *Roland et al.*, 2015] and other studies that identified significant hysteretic behavior [*Barron-Gafford et al.*, 2011; *Hamerlynck et al.*, 2013; *Zhang et al.*, 2015] we ask (3) Can the GM method produce accurate subdaily F_{soil} measurements?

2. Measurements and Analyses

2.1. Experimental Site

This study was conducted at the Santa Rita Mesquite Savanna AmeriFlux site, south of Tucson, AZ, USA (31.821°N, 110.866°W), from 1 November 2014 to 31 October 2015. The climate is warm-winter steppe [*Köppen*, 1918] with a mean annual precipitation of approximately 380 mm. About 50% of the annual precipitation occur during the summer (July–September) with the driest months occurring between summer and winter [*Scott et al.*, 2009]. Mean annual temperature is 19°C, with maximum in the summer of ~40°C and minimum in winter ~5°C. The vegetation is dominated by an overstory of 3–4 m high *Prosopis velutina* (velvet mesquite) trees [*Wooton*, 1898], with a canopy cover about 35%, and an understory of perennial C_4 bunchgrasses and annual C_4 grasses, interspersed subshrubs, and succulents. The soil texture is a loamy sand of >2 m depth. The soil layers from 0–10 cm, 10–20 cm, 20–50 cm, and 50–80 cm contain approximately 0.73%, 0.46%, 0.26%, and 0.27% soil organic carbon and 0%, 0%, 35%, and 13% inorganic carbon and a root density of 0.0015 g cm^{-3}, 0.0014 g cm^{-3}, 0.0005 g cm^{-3}, and 0.0001 g cm^{-3}, respectively. More details of the site can be found in *Scott et al.* [2009, 2015].

2.2. Soil CO_2 Measurements from Chambers and Profiles

Two automated soil CO_2 efflux chambers with soil collars inserted 8 cm into the ground were installed under the canopy of two mesquite trees (located 5 m apart) and controlled by a multichamber monitoring system (LI-8100, LI-COR, Lincoln, NE, USA). This system was programmed to monitor chamber air temperature, relative humidity, CO_2 molar fraction, and atmospheric pressure every second during 90 s measurement intervals every 2 h. F_{soil} was obtained using the LI-8100 software, and chamber runs where the model fit had a regression coefficient (R^2) less than 0.9 were rejected from analysis, representing <1% of the total data. Close to each chamber, two CO_2 sensors with a range of 0–5000 ppm, accuracy ±1.5% of the range, and ±2% of the reading (GMM-222, Vaisala Inc., Finland); two soil thermistors (107, Campbell Scientific, Logan, UT, USA; hereafter CSI); and two soil moisture probes installed horizontally (CS616, CSI) were installed at 10 cm depth.

One final CO_2 sensor and thermistor were installed at 2 cm above the soil, in a radiation shield to avoid direct solar radiation, and measured the atmospheric CO_2 molar fraction and air temperature. Measurements were made every 30 s with all sensors and stored as 30 min averages by a data logger (CR1000, CSI). For this paper, 2 h averages of the above variables were used. Approximately every month the probe calibration was checked [*Hamerlynck et al.*, 2013]. There were two significant gaps in the measurements (23 December to 13 March and 3–15 May) due to chamber malfunction or when the batteries were stolen. The two data gaps were simply excluded from our cumulative annual flux estimates. As an estimate of the uncertainty in the chamber F_{soil}, we report the mean and the range between both chambers.

2.3. Interwell SF_6 Pulse Injection

Nine injection profiles were installed in the soil near the chambers and CO_2 profiles. Every SF_6 profile was composed of three stainless steel tubes (9.5 mm outside diameter (OD) and 8.1 mm inside diameter) filled with a threaded rod (7.9 mm OD) at 5, 10, and 20 cm depth. Perforations were made at the bottom of the steel tube, and the top was connected and sealed with a stopcock fitting. The 20 cm tube was used as the injection well, and the gas was sampled using the tubes at 5 and 10 cm. We injected 5 mL of air containing atmospheric air with 16 ppm of SF_6 in the injection well. At 3 min intervals, six 10 mL samples were extracted from both depths and analyzed within 24 h. We used a gas chromatograph (8610 SRI Instrument, USA) outfitted with a 1 mL injection loop (1.8 m × 3.175 mm Haysep D column) followed by a 30 cm × 3.175 mm Mol Sieve 5A column, and electron capture detector, similar to the protocol described by *Johnson et al.* [1998]. Five sampling campaigns were conducted to measure the diffusion rate at various soil water contents. The driest campaign was on 28 July, and the other four campaigns were made after multiple rainy days (58 mm in 4 days; Figure 1) on 25, 27, and 29 September and 1 October.

2.4. Determination of Diffusion Coefficient (D_s), Transfer Coefficient (k_s), and F_{soil}

Equations and soil information of published 14 D_s empirical models and 2 in situ models consisting of (1) a k_s model, hereafter referred to as "Chamber model," obtained using a calibration between the chamber and the gradient method (GM), and (2) a D_s model, hereafter referred to as "SF_6 model," obtained through interwell pulse injection, are given in Table 1.

2.4.1. F_{soil} Determination Through the GM Using the Diffusion Coefficient (D_s)

The GM estimates soil CO_2 effluxes assuming that all the transport is due to diffusion processes through the equation [*Kowalski and Argueso*, 2011]

$$F_{(x)} = -\rho D_s \frac{\partial c}{\partial x} \quad (1)$$

where $F(x)$ is the F_{soil} at depth × (μmol CO_2 m^{-2} s^{-1}), D_s is the soil CO_2 diffusion coefficient (m^2 s^{-1}), ρ is the mean air density (mol air m^{-3}), ∂c is the CO_2 molar fraction gradient (μmol CO_2 mol air^{-1}), and ∂x is the vertical gradient (m).

D_s was obtained by published 14 D_s empirical models, and in the in situ SF_6 model, ∂c values were obtained as the difference between CO_2 molar fractions in the atmosphere and at 10 cm depth; ∂x was 0.1 m, and ρ was obtained from the ideal gas law.

#### 2.4.2. k_s Determination Using a Soil CO_2 Chamber and CO_2 Sensors

Estimates of soil CO_2 effluxes through the GM are not only sensitive to diffusive transport but also to nondiffusive transport and production/consumption processes that can occur in the soil layer, through this equation:

$$F_{(x)} = -\rho k_s \frac{\partial c}{\partial x} \quad (2)$$

where k_s is an empirical CO_2 transfer coefficient in m^2 s^{-1} that includes diffusive and nondiffusive transport and production or consumption processes that can occur in the studied layer. The term k_s is also known as an apparent diffusivity (D_{app} [*Roland et al.*, 2015]), and for this study was obtained by rearranging equation (2):

$$k_s = -\frac{F_{soil} \partial x}{\rho \partial c} \quad (3)$$

where F_{soil} values were obtained from the chamber measurements, ∂c values were obtained as the difference between CO_2 molar fractions in the atmosphere and at 10 cm depth, ∂x was 0.1 m, and ρ was obtained from the ideal gas law.
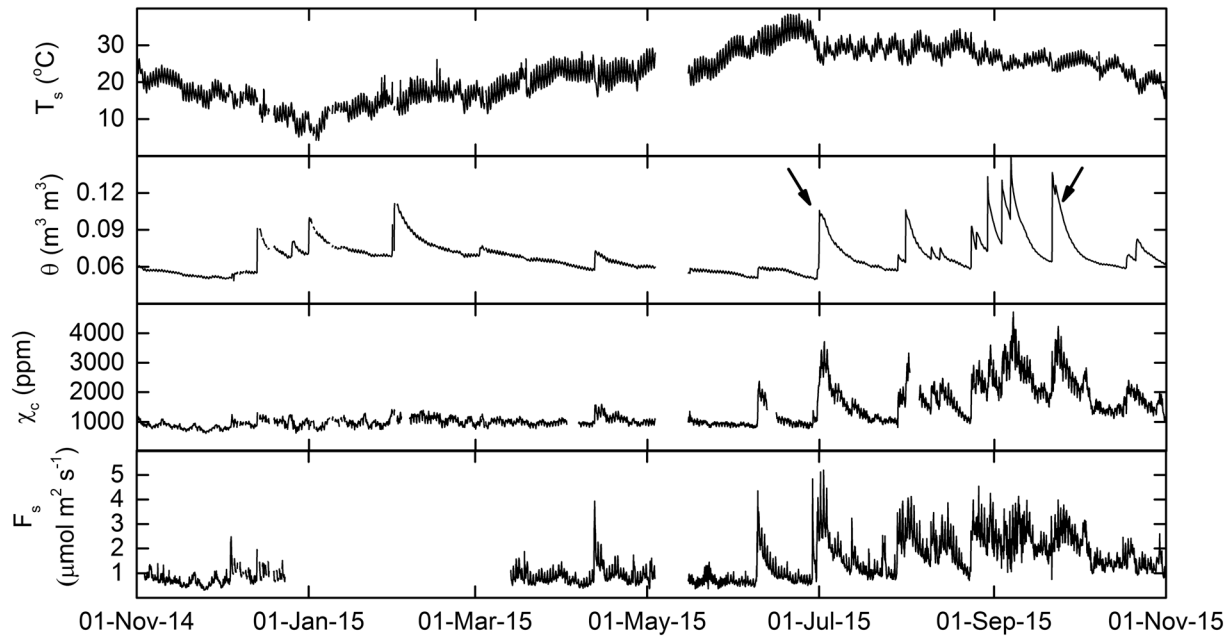
Figure 1. Average of soil temperature (T_s; $n = 4$), volumetric water content (θ; $n = 2$), CO_2 molar fraction (χ_c; $n = 4$), all of them at 10 cm depth, and average of soil CO_2 efflux (F_{soil}; $n = 2$) measured from chambers. The black arrows indicate the two rain pulses over which subsetted data were used for separate GM calibration.

2.4.3. D_s Determination Through Interwell SF_6 Pulse Injection

D_s was calculated with the equation proposed by *Werner et al.* [2004] for the interwell method with an instantaneous point source:

$$D_s = \left(\frac{\theta_a r^2}{6 f_a t_{max}} \right) \left(\frac{D_a}{D_{SF6}} \right) \tag{4}$$

where θ_a is the air-filled porosity ($m^3\,m^{-3}$) obtained as the soil porosity (Φ) minus the volumetric soil water

Table 1. Soil Diffusion Equations and the Porous Material That They Were Developed for[a]

Authors	Model	Porous Material
Buckingham [1904]	$D_s = D_a \theta_a^2$	Repacked soils
Penman [1940]	$D_s = D_a 0.66\theta_a$	Different porous materials
Marshall [1959]	$D_s = D_a \theta_a^{3/2}$	Different porous materials. Equation derivate from *Marshall* [1957]
Millington [1959]	$D_s = D_a \theta_a^{4/3}$	Comparison of publish results
Millington and Quirk [1961]	$D_s = D_a \frac{\theta_a^{10/3}}{\Phi^2}$	Different porous materials
Currie [1970]	$D_s = D_a \left(\frac{\theta_a}{\Phi}\right)^4 \Phi^{3/2}$	Sand
Lai et al. [1976]	$D_s = D_a \theta_a^{5/3}$	Undisturbed and repacked soils. Sandy loam
Sadeghi et al. [1989]	$D_s = D_a 0.18 \left(\frac{\theta_a}{\Phi}\right)^{2.98}$	Soils with clay content from 10.3 to 51.1%
Xu et al. [1992]	$D_s = D_a \frac{\theta_a^2}{\Phi^2}$	Silty clay loam soils
Moldrup et al. [1997]	$D_s = D_a 0.66\theta_a \left(\frac{\theta_a}{\Phi}\right)^{\frac{12-m}{3}}$	Undisturbed and repacked soils. $m = 3$ for undisturbed
Moldrup et al. [1999]	$D_s = D_a \Phi^2 \left(\frac{\theta_a}{\Phi}\right)^{\beta S}$	Undisturbed soils
Moldrup et al. [2000]	$D_s e D_a \frac{\theta_a^{2.5}}{\Phi}$	Repacked soils ranged from 6 to 54% clay
Jabro et al. [2012]	$D_s = D_a 0.98\theta_a^{1.315}$	Sandy loam
Ghanbarian-Alavijeh and Hunt [2012]	$D_s = D_a \left(\frac{\theta_a - \varepsilon_t}{1 - \varepsilon_t}\right)$	Different porous materials
Sánchez-Cañete [2016] Chamber model	$k_s = D_a 11.62\theta_a^{3.05}$	Loamy sand
Sánchez-Cañete [2016] SF_6 model	$k_s = D_a 4.97\theta_a^{2.56}$	Loamy sand

[a]D_s is the CO_2 diffusion coefficient, D_a is the diffusion coefficient of the CO_2 in free air, k_s is the CO_2 transfer coefficient, Φ is the soil porosity, θ_a is the soil air porosity (=Φ − soil water content), $\beta = 2.9$ is for sandy and clayey soils, $S = 0.948$ is the percent of mineral soil with particle size $>2\,\mu m$, and $\varepsilon_t = 0.1\Phi$ is the critical value for percolation in the porous medium.

content (θ; cm^3 cm^{-3}), r is the distance from the point source (m), f_a is the fraction of the injected mass of SF$_6$ conserved in the soil air ($f_a = 1$), t_{max} is the time of the maximum SF$_6$ concentration (s), and D_a is the diffusion coefficient of CO$_2$ in free air (m^2 s^{-1}). Φ was calculated from soil bulk density (ρ_b) and particle density (ρ_d) data as $\Phi = 1 - (\rho_b/\rho_d)$, resulting in 0.38 cm^3 cm^{-3} for our site. D_{SF6} is the diffusion coefficient of the SF$_6$ in free air (m^2 s^{-1}), both calculated following *Jones* [1992]:

$$D_a = D_{a,0} \left(\frac{T}{T_0}\right)^{1.75} \left(\frac{P}{P_0}\right) \qquad (5)$$

$$D_{SF6} = D_{SF6,0} \left(\frac{T}{T_0}\right)^{1.75} \left(\frac{P}{P_0}\right) \qquad (6)$$

where $D_{a,0}$ is $1.47°10^{-5}$ m^2 s^{-1}, $D_{SF6,0}$ is $0.89°10^{-5}$ m^2 s^{-1}, T_0 is 293.15 K, P_0 is 101,325 Pa, and T and P are the temperature (K) and pressure (Pa), respectively. Through equation (4), the diffusion coefficients for the layer 10–20 cm and the layer 5–20 cm were obtained, D_{s10-20} and D_{s5-20}, respectively. D_s from 0 to 10 cm (D_{s0-10}) was calculated by

$$D_{s0-10} = \left(\frac{D_{s5-20} - D_{s20-10}}{\partial_r}\right) \cdot \partial_x \qquad (7)$$

where ∂_r is the difference between the distances from the point source and the sampling tubes (m) and ∂_x is the soil layer thickness (*m*; 0.1 in our case).

### 2.4.4. Modeling D_s and k_s in Function of Soil Air Porosity

To obtain the diffusion and the gas transfer models, D_s and k_s were fit using a power function ($y = D_a ax^b$) of the soil air porosity (θ_a), where y is the D_s or k_s, D_a is the diffusion coefficient of CO$_2$ in free air (m^2 s^{-1}), x is θ_a, and a and b are the coefficients obtained by least squares regression. Two in situ models were obtained: (1) the Chamber model based on the k_s obtained during the whole period (equation (3)) and (2) the SF$_6$ model based on the D_s obtained from the five campaigns (equation (4)). Four additional k_s models were obtained using shorter, subsetted monitoring periods based on two rain pulses at the beginning and end of the summer rainy season (2–22 July and 23 September to 14 October). Two of these four additional models were obtained using all the variables monitored continuously at the maximum frequency (every 2 h, July pulse and September pulse), and the other two models only used one daily measurement at 10:00 A.M. during these pulse periods (daily July and daily September). The time of 10:00 A.M. is arbitrary but chosen to simulate a field visit to take one measurement with a portable chamber. Also, a bootstrap analysis with 10,000 iterations was employed to take random samples at any hour with 5 different sampling frequencies of F_{soil} (1 sample every 2 months and 1, 2, 3, or 4 samples per month) to simulate infrequent manual chamber measurements and determine the uncertainty in the resultant cumulative F_{soil} estimates due to the different sampling strategies.

3. Results

The F_{soil} and CO$_2$ molar fraction (χ_c) at 10 cm varied significantly at short temporal scales, driven mainly by rain pulses (Figure 1). During this period, the 10 cm soil temperature showed an annual pattern with a mean of 22.4°C, a maximum in July (38.5°C), and minimum in January (4.3°C). Soil water content ranged between 0.15 m^3/m^3 after rains and 0.05 m^3 m^{-3} prior to summer monsoon (July). Over the yearlong period, the soil χ_c at 10 cm averaged 1342 ppm with a maximum in July (4725 ppm) and a minimum in January (603 ppm). Soil CO$_2$ effluxes measured with the chambers showed a similar pattern to the soil χ_c, with a mean value of 1.39 µmol m^2 s^{-1}, a maximum in July of 5.20, and a minimum in January 0.32 µmol m^2 s^{-1}.

At a given soil air porosity, we found large differences in the relative diffusion coefficient (D_s/D_a) and the relative gas transfer coefficient (k_s/D_a) for the 14 published D_s models and our 2 in situ models (Figure 2). The Chamber model yielded a higher k_s/D_a at a given soil air porosity than the D_s/D_a values in the SF$_6$ model, and therefore, k_s was always higher than D_s. All published models, except that of *Xu et al.* [1992], underestimated the relative diffusion coefficient determined in situ at this site (SF$_6$ model). The equations and fitting parameters for these two in situ models can be found in Table 2 (Chamber model and SF$_6$ model).

After 1 year of near-continuous data, we found very large differences in the cumulative F_{soil} for the different diffusion and transfer models compared to the measured soil efflux (Figure 3a). The Chamber model showed
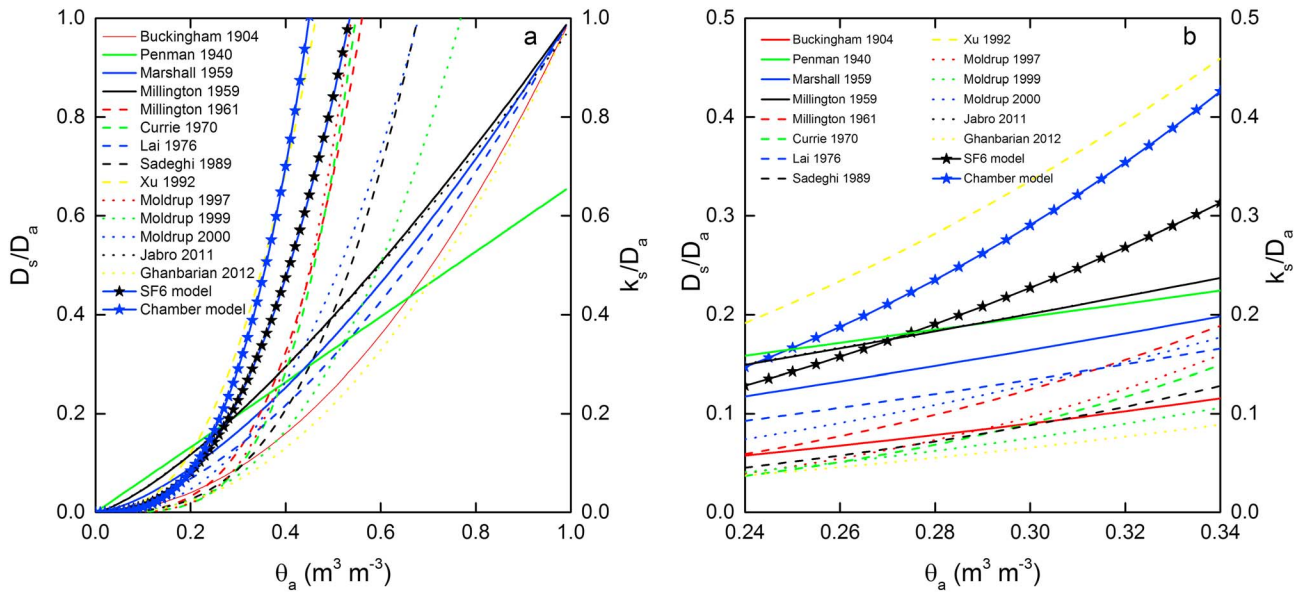
Figure 2. Relative CO_2 diffusion coefficient (D_s/D_a) for 14 published empirical models and the SF_6 model (black stars) and the relative CO_2 transfer coefficient (k_s/D_a) obtained by the Chamber model (blue stars), including the (a) whole possible range of soil air porosity (θ_a) and for the (b) range of soil air porosity found in this study.

the best agreement with the mean soil efflux (343 and 345 g C m^{-2}, respectively; <0.6% error). The SF_6 model CO_2 flux summed to 260 g C m^{-2}, an underestimation of 32%. With the exception of *Xu et al.* [1992] (383 g C m^{-2}; 10% overestimation), all published models underestimated the CO_2 flux by 55% to 361% (222 g C m^{-2} to 75 g C m^{-2}, respectively).

Four CO_2 transfer models (k_s) derived from short monitoring periods around two rain pulses at the beginning and end of the monsoon season (2 July and 23 September; see arrows in Figure 1) used with the GM showed good cumulative soil efflux estimates, falling within the range of measured soil effluxes (Figure 3b). The cumulative F_{soil} obtained from the two k_s models obtained using all the variables monitored every 2 h (July pulse and September pulse) underestimated the mean of the chamber efflux by 4.8% and 9.0% using the July and September pulses, respectively. The range of soil water content for the July pulse (0.06–0.1) represented 41.3% of the annual range versus 57.8% (0.06–0.12) for the September pulse. The other two models based on one daily measurement during the pulse event resulted in a 1.6% overestimation during July and a 4.8% underestimation during September (Figure 3b). The equations and fitting parameters for all in situ models can be found in Table 2. More statistical information comparing 2 week cumulative F_{soil} and the cumulative F_{soil} estimated by the other D_s and k_s models are shown in the Figure S1 in the supporting information. We assumed a 10% uncertainty in the SF_6 injector-sampling distance, and this assumption resulted in a cumulative CO_2 efflux that falls within the range of measured soil effluxes (overlapping shadow areas in Figure 3b). Considering all k_s model estimates, only the SF_6 model and one D_s model [*Xu et al.*, 1992] produced estimates that were within the range of the chamber CO_2 efflux measurements.

**Table 2.** Equations for the Derived CO_2 Transfer Models[a]

Model	Equations	R^2	RMSE	Samples	F Value	p Value F	p Values Coeff.1–2	Range θ_a	RMSE Validation Data
Chamber model	$k_s = D_a 11.62\theta_a^{3.05}$	0.24	0.08	4,380	28,790	<0.01	<0.01, <0.01	0.23–0.33	-
SF_6 model	$k_s = D_a 4.97\theta_a^{2.56}$	0.85	0.02	5	451	<0.01	0.264, 0.026	0.26–0.32	-
July pulse	$k_s = D_a 8.71\theta_a^{2.84}$	0.23	0.05	240	877	<0.01	0.016, <0.01	0.28–0.32	0.08
Daily July	$k_s = D_a 5.45\theta_a^{2.39}$	0.41	0.03	20	3,724	<0.01	0.236, <0.01	0.28–0.32	0.08
September pulse	$k_s = D_a 4.14\theta_a^{2.24}$	0.51	0.03	264	926	<0.01	<0.01, <0.01	0.26–0.32	0.09
Daily September	$k_s = D_a 4.73\theta_a^{2.32}$	0.56	0.03	22	10,743	<0.01	0.110, <0.01	0.26–0.32	0.08

[a]Soil air porosity (θ_a = soil porosity − soil water content). D_a is the diffusion coefficient of the CO_2 in free air. k_s is the soil CO_2 transfer coefficient. The coefficient of determination (R^2), root-mean-square error (RMSE), number of samples, F statistic, p values, range of soil air porosity, and RMSE validated with the whole database are also given.
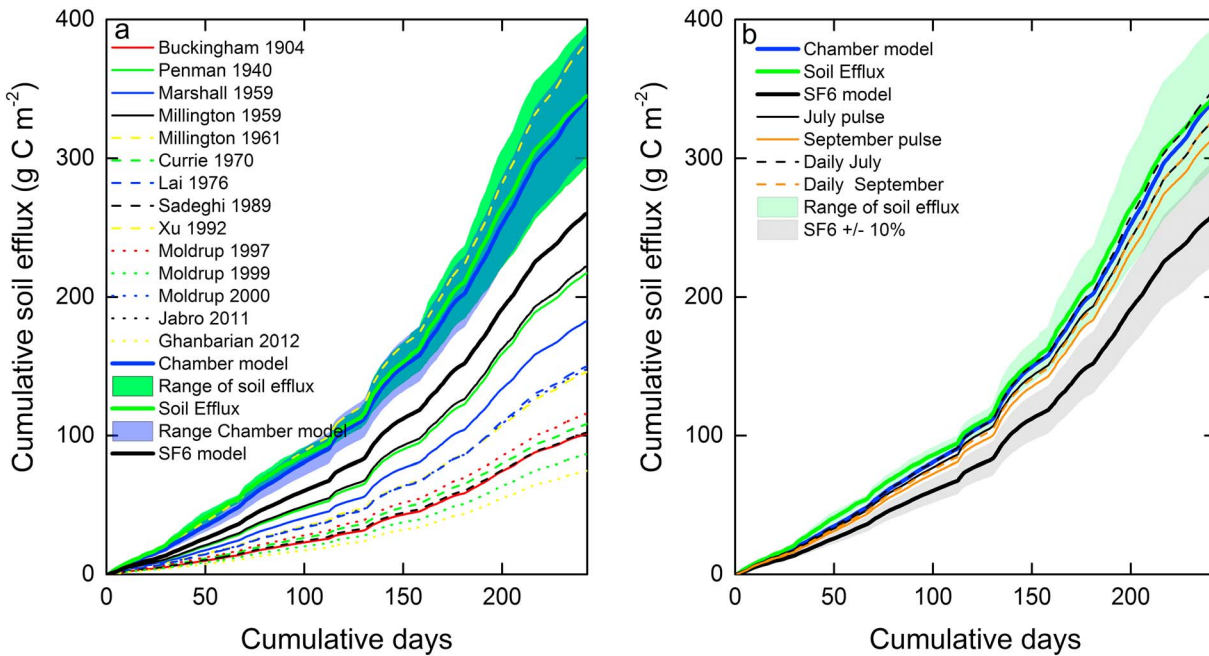
Figure 3. Over the whole period of available data: (a) cumulative F_{soil} for 14 published empirical models, SF$_6$ model, Chamber model, and its range at 95% confidence interval and mean soil efflux from the chamber and its range. (b) Cumulative F_{soil} for the soil efflux chamber and its range, SF$_6$ model $\pm$ 10% of error in the injector-sampling distance, Chamber model (obtained using the whole monitoring period), and four models based on two rain pulses (July and September) with continuous monitoring of the F_{soil} or with only one daily measurement per day during the rain pulse considered.

An increase of the sampling frequency yielded a decrease of uncertainty in the estimates of cumulative F_{soil} due to a better calibration of the k_s model (Figure 4). Errors below $\pm5\%$ were found in 82%, 77%, 76%, 65%, and 56% of the k_s models obtained with a frequency of 4, 3, 2, 1, and 0.5 samples per month, respectively. The mean and standard deviation of the absolute difference between cumulative sums were $7.5 \pm 5.4\%$ for one sample every 2 months, $5.5 \pm 4.1\%$ for one sample per month, $4.2 \pm 3.2\%$ for two samples per month, $3.7 \pm 2.7\%$ for three samples per month, and $3.3 \pm 2.5\%$ for four samples per month.
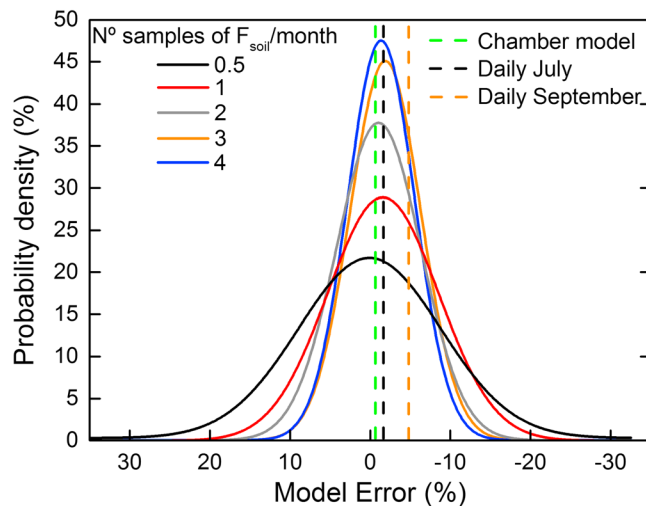
Figure 4. Probability density function of error between the cumulative F_{soil} measured by chambers and estimated from 10,000 CO$_2$ transfer coefficient (k_s) models at 5 different sampling frequencies (continuous lines). The vertical dashed lines show the errors obtained with some previous models: Chamber model 0.6%, daily July 1.6%, and daily September 4.8%. Model error $(\%) = \frac{\left| \Sigma F_{soil}^{meas} - \Sigma F_{soil}^{model} \right|}{\Sigma F_{soil}^{meas}} \times 100.$
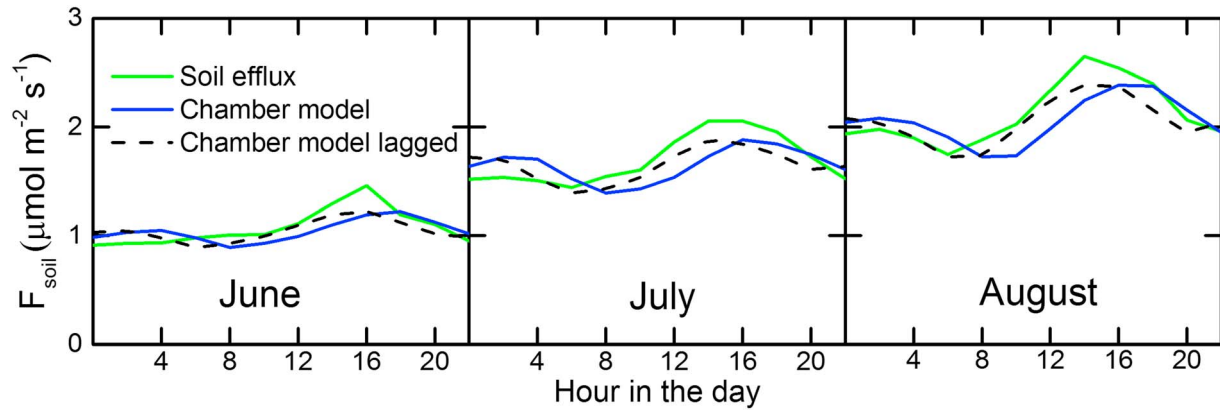
Figure 5. Monthly average diurnal of soil CO_2 efflux (F_{soil}) obtained with the automatic chamber (green), the Chamber model (blue), and the Chamber model lagged 2 h (black dashed line) during the months of June, July, and August.

When the GM is applied, there is a lag between the daily maximum and minimum F_{soil} obtained by the automatic chamber and the GM using the Chamber model (Figure 5). A cross-correlation analysis determined a 2 h lag based on surface temperature and 10 cm depth temperature, and this lag was applied to the F_{soil} estimated by the GM. This improved the comparison of the subdaily measurements (Figure 5) with the coefficients of determination (R^2) for monthly averaged diurnal fluxes, where the R^2 between F_{soil} and the Chamber model were 0.47, 0.34, and 0.53 during June, July, and August, respectively, and 0.68, 0.62, and 0.83 from F_{soil} and the Chamber model lagged 2 h. During the whole study period the coefficient of determination between the raw diurnal F_{soil} and the Chamber model was 0.80, and with the lag applied it was 0.82.

The relatively low R^2 found between the soil air porosity and the gas transfer coefficient (k_s) indicated that variables other than soil water content were influencing k_s (Table 2). This may also indicate that nondiffusive transport mechanisms were involved. To study the wind effect on k_s, the whole database was stratified, discerning between "windy days," days with daily mean of wind speed $>3.5 \, \text{m s}^{-1}$, and "calm days" with daily mean of wind speed $<1.6 \, \text{m s}^{-1}$, equivalent to 90th and 10th percentile, respectively. During windy days, the fitting between soil air porosity and k_s was much poorer (standard error of the regression, $S = 0.089$; Figure 6) than during calm days ($S = 0.049$). The k_s model obtained for windy days underestimated the cumulative F_{soil} by 2.3% during the whole year; however, the k_s model obtained for calm days overestimated the cumulative F_{soil} by 6.7%.
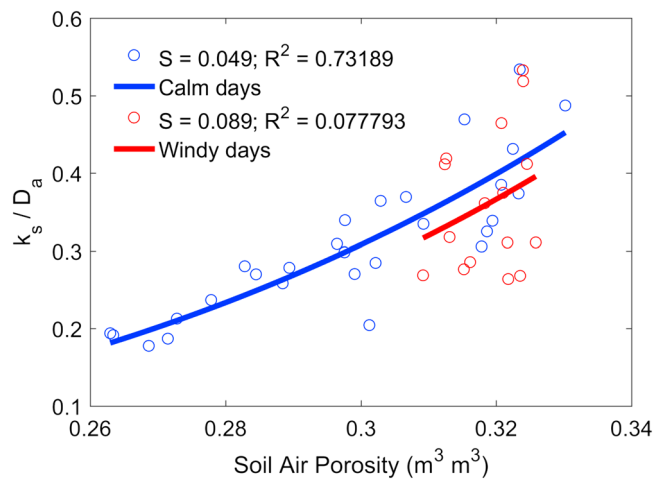
Figure 6. Relative CO_2 transfer coefficient (k_s/D_a) versus soil air porosity for calm days (blue dots; $n = 28$) and windy days (red dots; $n = 16$). The standard error of the regression (S) and coefficient of determination (R^2) are given from the fitting at a power function ($y = D_a \, ax^b$).

4. Discussion

An accurate quantification of F_{soil} across ecosystem flux measurement sites would help to resolve the role that this component flux plays in the net ecosystem carbon balance and its dominant controls. Unfortunately, separate F_{soil} estimates are rarely available as automated chamber systems are typically expensive and difficult to maintain. The gradient method is attractive due to its simpler design and lower cost, but the accuracy of the method is questionable because of the use of off-the-shelf published models for the diffusion coefficient. Herein, we have addressed three questions whose answers lead to new best practices in the application of the GM technique.

4.1. Which Method Produces the Best Estimate of Cumulative F_{soil}?

The most accurate long-term F_{soil} measurements were obtained by using an empirical soil CO_2 transfer coefficient in situ (Chamber model) applied to the GM, which produced only a 0.6% difference on cumulative F_{soil} measured by soil chambers. We found that published D_s models and the in situ D_s model that was obtained using the tracer injection technique did not result in very accurate cumulative F_{soil} estimates; rather, the Chamber k_s model showed the best agreement with the F_{soil}. At our experimental site, 93% (13 of 14) of published D_s models used with the GM method produced unsuitable F_{soil} estimates, as compared to our measurements with the automated chambers (Figure 3a). This result supports the need to determine D_s in situ at any experimental site, as suggested by *Pingintha et al.* [2010] and *Roland et al.* [2015]. The most common way to determine D_s is ex situ, either collecting undisturbed core samples in the field [*Moldrup et al.*, 1996] or collecting soil samples and repacking them [*Moldrup et al.*, 2000] to later test in laboratory. The main problem of ex situ determinations is that this methodology is very likely to disturb the soil structure during extraction and transport. Both in situ and ex situ published models yield large uncertainties when used in other soils, simply because these models were developed for specific soil conditions based mainly on soil porosity and water content (Table 1). Soil porosity can vary widely between soil layers especially in the upper horizon (in our case, the first few centimeters) due to the organic matter content, which changes bulk density and so affects porosity. The soil porosity has an important effect in the diffusion models (Figure 2); therefore, an accurate determination of this parameter in the studied layer is essential when ex situ diffusion models are used. In the same way, it is very complicated to obtain a water content estimation that is representative of the shallow soil layer, since sensors that integrate a particular soil volume are sensitive to differences in soil mineralogy [*Vaz et al.*, 2013] and can be influenced by the soil-atmosphere interface when installed at shallow depths. The soil volume measurements vary depending on the probe installation position either in horizontal, vertical, or at angle, with the angle position being the most adequate to determine the soil water content in the layer of interest.

All of these uncertainties in the determination of the soil porosity, insertion strategy, and probe calibration could have contributed to the error magnitude of the 14 published empirical diffusion models. These uncertainties will be propagated to whatever D_s model chosen in future studies because these models are empirical in nature, and thus, they would not be expected to hold under all conditions. At this site and with this experimental design, we found a large underestimation when using 13 published empirical diffusion models. However, the magnitude of error in F_{soil} in the published models would be expected to decrease if CO_2 is measured at shallower depths because there would be less soil CO_2 production between the CO_2 measurement and the soil surface.

Differences in cumulative F_{soil} estimates between D_s models and k_s models (Figure 3) also could be due to the k_s models implicitly accounting for the diffusive and nondiffusive transport and production processes of CO_2 in the soil between sampling depths, whereas D_s models are subject to diffusion alone. When comparing both in situ gas transport models, the Chamber model implicitly accounted for the diffusive and nondiffusive transport and production processes of CO_2 in the soil between sampling depths, but the SF_6 model used a conservative tracer subject to diffusion alone. The classic gas diffusion models are based on a conservative tracer, assuming that all molecules are conserved in the soil air, neglecting production or consumption processes. Although there are differences in solubility in water between SF_6 and CO_2 (CO_2 approximately 30 times higher than SF_6 [*Wilhelm et al.*, 1977]), this contribution is usually neglected because diffusion of these gases in water is about 10,000 times lower than in the air [*Allaire et al.*, 2008].

Different models using conserved gases determine the diffusion coefficient for any gas of interest by using the ratio between the molecular diffusion coefficient (D_m) for the gas of interest and D_m for the conserved gas used [*Werner et al.*, 2004; *Allaire et al.*, 2008]. Therefore, the gas of interest also is treated as a conservative gas, which is not valid for soil gases like CO_2, CH_4, NO_x, N_2O, H_2S, and SO_2 that may be both produced or consumed as they move through the soil matrix. We would expect CO_2 production in the 0–10 cm layer, and for this reason, the SF_6 model likely underestimated CO_2 effluxes (Figure 3). Differences between SF_6 and Chamber models could also be due to two more reasons. First, we estimated D_s for the 10–20 cm and 5–20 cm depths and then extrapolated D_s to the 0–10 cm layer. If D_s decreases with depth, this would result to an underestimate of D_s from 0 to 10 cm. Second, the SF_6 method was only carried out 5 times, and this may have contributed to a regression that was not statistically significant ($p = 0.264$; Table 2). While this may not necessarily create a bias, it limits our confidence in the relationship between water content and diffusion. Finally, the CO_2 production of this layer plays an important role in the k_s models based on rain pulses. As expected, the July pulse (early monsoon) obtained higher values of cumulative annual F_{soil} than the September pulse (later monsoon) because soil effluxes for a given pulse size tend to be larger at the onset of rains versus later in a rainy season [*Franzluebbers et al.*, 2002; *Sponseller*, 2007; *Vargas et al.*, 2012].

4.2. Can We Use a Limited Set of Soil CO_2 Effluxes Over a Rain Pulse to Produce an Accurate Cumulative Efflux Estimate?

Gas transfer models based on continuous soil efflux measurements, or more simply by a once-a-day measurement that follows a soil water dry-down event (i.e., to simulate sampling with a portable chamber), produce better estimates of F_{soil} than any published empirical diffusion model (Figure 3b). Comparing a limited set of measurements, we found that gas transfer models derived from the daily measurement at 10:00 A.M. resulted in even a slightly better estimation of cumulative F_{soil} than models using continuous measurements, but, more importantly, all pulse models were better than the SF_6 model and the published empirical diffusion models (Figure 3b). The slightly better estimation of cumulative F_{soil} in the models derived from one daily measure than the models using continuous measurements over the same pulses is simply a coincidence due to chosen 10:00 A.M. sampling time. Alternative models derived from a once daily measurement at a specific hour do not always result in a better estimation of cumulative F_{soil} than models using continuous measurement, but all of them fall within the cumulative efflux measurement range (Table S1 in the supporting information). The best cumulative F_{soil} estimations were derived from once daily samplings, resulting in a 0.8% overestimation (sampling at 04:00 A.M. during the July pulse) and a 1.2% underestimation (06:00 A.M., September pulse); the worst F_{soil} estimations resulted in a 17.3% underestimation (16:00 P.M., July) and a 15.4% underestimation (18:00 P.M., September). Windy days underestimated F_{soil} (Figure 6). For this reason, we believe that the improved F_{soil} estimations using predawn sampling time (04:00–06:00) may be due to increased wind in the late afternoon (16:00–18:00). The efflux measurement range found between the chambers highlights probable measurement uncertainty due to the instrumentation as well as the likely heterogeneity in the soil CO_2 effluxes (Figure 3) due to micrometeorological conditions, such as differences in shading, as well as differences in soil properties and root density.

For future studies working with the gradient method, we recommend taking at least one F_{soil} manual chamber measurement per month over the largest range of soil water content possible. Seasonality is captured in the CO_2 gradient through time; combined with measures of F_{soil} by the manual chamber that can capture a range of environmental conditions, revised F_{soil} estimates by the GM will be significantly improved. Given similar conditions to our study, this would allow the building of a k_s model that would yield yearly F_{soil} estimates within 5.5% of the mean between the absolute difference between F_{soil} estimated and F_{soil} obtained from chamber measurements. However, as the bootstrap analysis showed, an increase in the sampling frequency would yield better calibrated k_s models and therefore better F_{soil} estimates (Figure 4).

4.3. Can the GM Method Produce Accurate Subdaily F_{soil} Measurements?

We have shown that accurate F_{soil} estimations can be obtained by the GM at daily to seasonal scales, but it is necessary to correct for an apparent lag associated with the measurement depth to improve the agreement at subdaily scales. A schematic drawing of the diurnal patterns of temperature, soil CO_2 molar fraction, and F_{soil} measured by the chamber and F_{soil} obtained by the gradient method at different depths are shown in Figure S2. This decoupling between the F_{soil} measured by the chamber and the F_{soil} estimated by the GM

at different depths occurs because the time to reach the maximum CO_2 molar fraction is delayed at deeper depths, just like soil temperature. Previous studies have identified significant hysteretic behavior [*Barron-Gafford et al.*, 2011; *Hamerlynck et al.*, 2013; *Zhang et al.*, 2015] associated with lags between CO_2 production and soil temperature [*Vargas et al.*, 2010], and we have attempted to systematically correct for these by following a technique widely used in eddy-covariance studies to determine the lag between variables [*Finkelstein and Sims*, 2001; *Langford et al.*, 2015]. Just as the GM is based on the difference between the mole fraction at one depth and the atmosphere, the deeper the sensor is, the greater the delay with respect to F_{soil} at the surface is. To correct for this lag, we used a cross-correlation analysis to determine the lag between surface temperature and the temperature at the depth of interest and we applied it to delay the F_{soil} series. At our experimental site, the cross-correlation analysis resulted on a 2 h lag and after applying it, on the series of F_{soil} obtained by the GM using the Chamber model, produced subdaily estimates in phase with the soil effluxes (Figure 5).

In contrast, *Roland et al.* [2015] found that none of their F_{soil} models were able to suitably predict the F_{soil} variations at the subdaily time scale. They suggest that this was likely due to the lack of large diurnal soil CO_2 variations which might have been due to more wind-driven advective transport [*Hirsch et al.*, 2004; *Maier et al.*, 2010; *Sanchez-Canete et al.*, 2011]. Our results showed that during calm days, the explained variance between soil air porosity and k_s was greatly improved with respect to windy days ($S = 0.049$ and $S = 0.089$, respectively; Figure 6). This suggests that nondiffusive transport induced by the wind contributed to a high source of noise in our data, justifying the low R^2 found with our Chamber model (Table 2). On the other hand, *Goffin et al.* [2015] did not find evidence that turbulence-induced transport could explain the poor agreement in subdaily F_{soil} and recommended that the focus should be placed on other factors affecting the CO_2 production. However, the failure in their simulated subdaily F_{soil} could be due to the application of a diffusion coefficient in the GM rather than an in situ determined transfer coefficient that implicitly can account for the CO_2 production in the soil layer.

The application of GM considering diffusion processes exclusively and neglecting nondiffusive ones leads to several sources of error that may contribute to differences on F_{soil} with respect to chamber measurements. Research on nondiffusive transport has found that the main drivers are wind, fluctuations in atmospheric pressure, soil-atmosphere thermal gradient, or air density associated with its composition. Numerous authors have found that advective transport driven by the wind can provoke changes in the soil CO_2 molar fraction [*Drewitt et al.*, 2005; *Seok et al.*, 2009; *Bowling and Massman*, 2011; *Goffin et al.*, 2014], soil CO_2 effluxes [*Subke et al.*, 2003; *Risk et al.*, 2013; *Roland et al.*, 2015], or in the atmosphere [*Kowalski et al.*, 2008; *Sanchez-Canete et al.*, 2011; *Nachshon et al.*, 2012; *Rey et al.*, 2012]. Nondiffusive transport has been associated both with small changes in pressure induced by the wind, commonly called pressure pumping [*Massman et al.*, 1997; *Takle et al.*, 2004; *Maier et al.*, 2010], or from synoptic atmospheric pressure changes [*Rogie et al.*, 2001; *Fujiyoshi et al.*, 2010; *Comas et al.*, 2011; *Sanchez-Canete et al.*, 2013b]. The soil-atmosphere thermal gradient also can generate convective transport provoking the exchange of the air between soil and atmosphere, both in fractures [*Weisbrod et al.*, 2009; *Moore et al.*, 2011] and in caves [*Serrano-Ortiz et al.*, 2010]. Finally, other nondiffusive transport processes are due to the effects on soil air buoyancy that result from the added density in the soil pore space air associated with CO_2 enrichment in the root zone [*Kowalski and Sanchez-Canete*, 2010; *Sanchez-Canete et al.*, 2013a]. All of these nondiffusive transport mechanisms can generate important errors in the gradient method depending on their magnitudes.

4.4. Importance of Accurate Long-Term Soil Efflux Measurements in Ecosystem Studies

Although F_{soil} represents a significant source of terrestrial CO_2 emissions [*Raich and Schlesinger*, 1992], continuous measurements of this important land-atmosphere exchange are only sparsely available despite a call from national ecosystem flux networks [*McFarlane et al.*, 2014]. At the ecosystem scale, the measurement of net ecosystem CO_2 exchange (NEE) can be partitioned into ecosystem respiration (R_{eco}) and gross ecosystem production (GEP) by temperature-sensitive, model-based estimates using the nighttime NEE data [*Falge et al.*, 2001; *Stoy et al.*, 2006; *Mahecha et al.*, 2010]. Despite advances on the net ecosystem CO_2 exchange (NEE) partitioning [*Desai et al.*, 2008], there are large uncertainties of NEE mainly associated to low-turbulence conditions at night, and these uncertainties are transferred to the partitioning of NEE into ecosystem respiration (R_{eco}) and gross ecosystem production (GEP) [*Barr et al.*, 2013]. Furthermore, R_{eco} consists of a belowground

component, F_{soil}, and an aboveground component attributed to plant respiration. F_{soil} is commonly measured manually, yielding a low sampling frequency, which translates into annual estimates that are highly uncertain (>99% of half-hour periods throughout a year for biweekly sampling) [*Gomez-Casanovas et al.*, 2013]. Therefore, comparative studies between F_{soil} at high resolution (spatially and temporally) and ecosystem fluxes are very useful to a better understanding about carbon cycle processes [*van Gorsel et al.*, 2008] and may influence on how we parameterize and construct models [*Vargas et al.*, 2011].

Although F_{soil} is generally the largest flux contributing to R_{eco}, few studies have compared both fluxes. Reported estimates of the relative contribution of F_{soil} to R_{eco} range between 48% and 71% found by *Lavigne et al.* [1997] at six coniferous boreal sites, 92% reported by *Longdoz et al.* [2000] in a mixed forest, 69% obtained by *Janssens et al.* [2001b] from 18 forest ecosystems, and 81% measured by *Knohl et al.* [2008] in an old beech forest. Only *Longdoz et al.* [2000] used continuous F_{soil} measures during the whole year; the other authors obtained annual F_{soil} from extrapolation of low-frequency measures using manual chambers. Clearly, the F_{soil} contribution is strongly dependent on the ecosystem and we need to produce accurate long-term estimates of F_{soil} across changing environmental conditions to improve our understanding of its contribution to R_{eco}.

5. Conclusions

An accurate depiction of CO_2 production and diffusion processes in soil is a key uncertainty in obtaining accurate measurements of F_{soil}. In this study, we found that the application of 13 out of 14 published diffusion models to the GM grossly underestimated (55%–361%) cumulative soil effluxes. An in situ diffusion model obtained by SF_6 injection also did not generate accurate estimations in cumulative F_{soil}, underestimating by 32%. Instead, we found great improvements by using the GM and chamber measurements to determine an empirical soil CO_2 transfer coefficient in situ (Chamber model), which produced nearly identical (0.6% difference) cumulative soil effluxes over 243 days. The difference between both in situ models could be a result of the Chamber model implicitly accounting for diffusive and nondiffusive transport, as well as including production of CO_2 in the soil layer, while the SF_6 model only accounts for diffusion processes.

Therefore, we recommend not using methodologies based on conservative tracers to build diffusion models that later will be applied in the GM. Rather, a long period of side-by-side measurements is the most appropriate way to build an in situ gas transfer model that is statistically more robust (more points to fit) and require less extrapolation outside of the soil water range. However, we found that a limited sampling of F_{soil} (e.g., using a portable chamber) can result in an adequate gas transfer model that generates accurate F_{soil} estimates. Therefore, we recommend that future F_{soil} studies use a combination of the GM and targeted manual or automatic F_{soil} chamber measurements to build the gas transfer model in situ and produce accurate long-term estimates of F_{soil}.

References

Allaire, S. E., J. A. Lafond, A. R. Cabral, and S. F. Lange (2008), Measurement of gas diffusion through soils: Comparison of laboratory methods, *J. Environ. Monit.*, 10, 1326–1336, doi:10.1039/b809461f.

Ball, B. C., C. A. Glasbey, and E. A. G. Robertson (1994), Measurement of soil gas diffusivity in situ, *Eur. J. Soil Sci.*, 45(1), 3–13, doi:10.1111/j.1365-2389.1994.tb00480.x.

Barr, A. G., et al. (2013), Use of change-point detection for friction-velocity threshold evaluation in eddy-covariance studies, *Agric. For. Meteorol.*, 171-172, 31–45, doi:10.1016/j.agrformet.2012.11.023.

Barron-Gafford, G. A., R. L. Scott, G. D. Jenerette, and T. E. Huxman (2011), The relative controls of temperature, soil moisture, and plant functional group on soil CO_2 efflux at diel, seasonal, and annual scales, *J. Geophys. Res.*, 116, G01023, doi:10.1029/2010JG001442.

Bond-Lamberty, B., and A. Thomson (2010), A global database of soil respiration data, *Biogeosciences*, 7(6), 1915–1926, doi:10.5194/bg-7-1915-2010.

Bowling, D. R., and W. J. Massman (2011), Persistent wind-induced enhancement of diffusive CO_2 transport in a mountain forest snowpack, *J. Geophys. Res.*, 116, G04006, doi:10.1029/2011JG001722.

Buckingham, E. (1904), *Contributions to Our Knowledge of the Aeration of Soils*, U.S. Dept. of Agriculture, Bureau of Soils, Washington, D. C.

Comas, X., L. Slater, and A. S. Reeve (2011), Atmospheric pressure drives changes in the vertical distribution of biogenic free-phase gas in a northern peatland, *J. Geophys. Res.*, 116, G04014, doi:10.1029/2011JG001701.

Currie, J. A. (1970), Movement of gases in soil respiration, in *Sorption and Transport Processes in Soils*, *Monogr. Soc. Chem. Ind.*, vol. 37, pp. 152–171, Soc. Chem. Ind., London.

Davidson, E. A., and I. A. Janssens (2006), Temperature sensitivity of soil carbon decomposition and feedbacks to climate change, *Nature*, 440(7081), 165–73, doi:10.1038/nature04514.

Davidson, E. A., and S. E. Trumbore (1995), Gas diffusivity and production of CO_2 in deep soils of the eastern Amazon, *Tellus Ser. B Chem. Phys. Meteorol.*, 47(5), 550–565, doi:10.3402/tellusb.v47i5.16071.

Davidson, E. A., K. E. Savage, S. E. Trumbore, and W. Borken (2006), Vertical partitioning of CO_2 production within a temperate forest soil, *Global Change Biol.*, *12*(6), 944–956.

Desai, A. R., A. D. Richardson, A. M. Moffat, J. Kattge, D. Y. Hollinger, A. Barr, E. Falge, A. Noormets, D. Papale, and M. Reichstein (2008), Cross-site evaluation of eddy covariance GPP and RE decomposition techniques, *Agric. For. Meteorol.*, *148*(6), 821–838.

Drewitt, G. B., T. A. Black, Z. Nesic, E. R. Humphreys, E. M. Jork, R. Swanson, G. J. Ethier, T. Griffis, and K. Morgenstern (2002), Measuring forest floor CO_2 fluxes in a Douglas-fir forest, *Agric. For. Meteorol.*, *110*, 299–317, doi:10.1016/s0168-1923(01)00294-5.

Drewitt, G. B., T. A. Black, and R. S. Jassal (2005), Using measurements of soil CO_2 efflux and concentrations to infer the depth distribution of CO_2 production in a forest soil, *Can. J. Soil Sci.*, *85*(2), 213–221.

Falge, E., et al. (2001), Gap filling strategies for defensible annual sums of net ecosystem exchange, *Agric. For. Meteorol.*, *107*, 43–69, doi:10.1016/s0168-1923(00)00225-2.

Finkelstein, P. L., and P. F. Sims (2001), Sampling error in eddy correlation flux measurements, *J. Geophys. Res.*, *106*(D4), 3503–3509, doi:10.1029/2000JD900731.

Franzluebbers, K., A. J. Franzluebbers, and M. D. Jawson (2002), Environmental controls on soil and whole-ecosystem respiration from a tallgrass prairie, *Soil Sci. Soc. Am. J.*, *66*(1), 254–262.

Fujiyoshi, R., Y. Haraki, T. Sumiyoshi, H. Amano, I. Kobal, and J. Vaupotic (2010), Tracing the sources of gaseous components (Rn-222, CO_2 and its carbon isotopes) in soil air under a cool-deciduous stand in Sapporo, Japan, *Environ. Geochem. Health*, *32*, 73–82, doi:10.1007/s10653-009-9266-1.

Ghanbarian-Alavijeh, B., and A. G. Hunt (2012), Comparison of the predictions of universal scaling of the saturation-dependence of the air permeability with experiment, *Water Resour. Res.*, *48*, W08513, doi:10.1029/2011WR011758.

Goffin, S., M. Aubinet, M. Maier, C. Plain, H. Schack-Kirchner, and B. Longdoz (2014), Characterization of the soil CO_2 production and its carbon isotope composition in forest soil layers using the flux-gradient approach, *Agric. For. Meteorol.*, *188*, 45–57, doi:10.1016/j.agrformet.2013.11.005.

Goffin, S., C. Wylock, B. Haut, M. Maier, B. Longdoz, and M. Aubinet (2015), Modeling soil CO_2 production and transport to investigate the intra-day variability of surface efflux and soil CO_2 concentration measurements in a Scots pine forest (*Pinus sylvestris* L.), *Plant Soil*, *1*, 195–211, doi:10.1007/s11104-015-2381-0.

Gomez-Casanovas, N., K. Anderson-Teixeira, M. Zeri, C. J. Bernacchi, and E. H. DeLucia (2013), Gap filling strategies and error in estimating annual soil respiration, *Global Change Biol.*, *19*, 1941–1952, doi:10.1111/gcb.12127.

Hamerlynck, E. P., R. L. Scott, E. P. Sanchez-Canete, and G. A. Barron-Gafford (2013), Nocturnal soil CO_2 uptake and its relationship to sub-surface soil and ecosystem carbon fluxes in a Chihuahuan desert shrubland, *J. Geophys. Res. Biogeosci.*, *118*, 1593–1603, doi:10.1002/2013JG002495.

Hirsch, A. I., S. E. Trumbore, and M. L. Goulden (2004), The surface CO_2 gradient and pore-space storage flux in a high-porosity litter layer, *Tellus Ser. B-Chem. Phys. Meteorol.*, *56*, 312–321, doi:10.1111/j.1600-0889.2004.00113.x.

Jabro, J. D., U. M. Sainju, W. B. Stevens, and R. G. Evans (2012), Estimation of CO_2 diffusion coefficient at 0–10 cm depth in undisturbed and tilled soils, *Arch. Agron. Soil Sci.*, *58*(1), 1–9, doi:10.1080/03650340.2010.506482.

Janssens, I. A., A. S. Kowalski, and R. Ceulemans (2001a), Forest floor CO_2 fluxes estimated by eddy covariance and chamber-based model, *Agric. For. Meteorol.*, *106*, 61–69, doi:10.1016/s0168-1923(00)00177-5.

Janssens, I. A., et al. (2001b), Productivity overshadows temperature in determining soil and ecosystem respiration across European forests, *Global Change Biol.*, *7*(3), 269–278, doi:10.1046/j.1365-2486.2001.00412.x.

Jassal, R., A. Black, M. Novak, K. Morgenstern, Z. Nesic, and D. Gaumont-Guay (2005), Relationship between soil CO_2 concentrations and forest-floor CO_2 effluxes, *Agric. For. Meteorol.*, *130*, 176–192, doi:10.1016/j.agrformet.2005.03.005.

Johnson, P. C., C. Bruce, R. L. Johnson, and M. W. Kemblowski (1998), In situ measurement of effective vapor-phase porous media diffusion coefficients, *Environ. Sci. Technol.*, *32*(21), 3405–3409, doi:10.1021/es980186q.

Jones, H. G. (1992), *Plants and Microclimate: A Quantitative Approach to Environmental Plant Physiology*, 2nd ed., Cambridge Univ. Press, New York.

Knohl, A., A. R. B. Søe, W. L. Kutsch, M. Göckede, and N. Buchmann (2008), Representative estimates of soil and ecosystem respiration in an old beech forest, *Plant Soil*, *302*(1-2), 189–202, doi:10.1007/s11104-007-9467-2.

Köppen, W. (1918), Klassifikation der Klimate nach Temperatur, Niederschlag und Jahresablauf (Classification of climates according to temperature, precipitation and seasonal cycle), *Petermanns Geogr. Mitt.*, *64*, 193–203.

Kowalski, A. S., and D. Argueso (2011), Scalar arguments of the mathematical functions defining molecular and turbulent transport of heat and mass in compressible fluids, *Tellus Ser. B-Chem. Phys. Meteorol.*, *63*, 1059–1066, doi:10.1111/j.1600-0889.2011.00579.x.

Kowalski, A. S., and E. P. Sanchez-Canete (2010), A new definition of the virtual temperature, valid for the atmosphere and the CO_2-rich air of the vadose zone, *J. Appl. Meteorol. Climatol.*, *49*, 1692–1695, doi:10.1175/2010jamc2534.1.

Kowalski, A. S., P. Serrano-Ortiz, I. A. Janssens, S. Sanchez-Moral, S. Cuezva, F. Domingo, A. Were, and L. Alados-Arboledas (2008), Can flux tower research neglect geochemical CO_2 exchange? *Agric. For. Meteorol.*, *148*, 1045–1054, doi:10.1016/j.agrformet.2008.02.004.

Lai, S.-H., J. M. Tiedje, and A. E. Erickson (1976), In situ measurement of gas diffusion coefficient in soils, *Soil Sci. Soc. Am. J.*, *40*, 3–6, doi:10.2136/sssaj1976.03615995004000010006x.

Langford, B., W. Acton, C. Ammann, A. Valach, and E. Nemitz (2015), Eddy-covariance data with low signal-to-noise ratio: Time-lag determination, uncertainties and limit of detection, *Atmos. Meas. Tech.*, *8*(10), 4197–4213, doi:10.5194/amt-8-4197-2015.

Lavigne, M. B., et al. (1997), Comparing nocturnal eddy covariance measurements to estimates of ecosystem respiration made by scaling chamber measurements at six coniferous boreal sites, *J. Geophys. Res.*, *102*, 28,977–28,985, doi:10.1029/97JD01173.

Longdoz, B., M. Yernaux, and M. Aubinet (2000), Soil CO_2 efflux measurements in a mixed forest: Impact of chamber disturbances, spatial variability and seasonal evolution, *Global Change Biol.*, *6*(8), 907–917, doi:10.1046/j.1365-2486.2000.00369.x.

Mahecha, M. D., et al. (2010), Global convergence in the temperature sensitivity of respiration at ecosystem level, *Science*, *329*(5993), 838–840, doi:10.1126/science.1189587.

Maier, M., and H. Schack-Kirchner (2014), Using the gradient method to determine soil gas flux: A review, *Agric. For. Meteorol.*, *192*, 78–95, doi:10.1016/j.agrformet.2014.03.006.

Maier, M., H. Schack-Kirchner, E. E. Hildebrand, and J. Holst (2010), Pore-space CO_2 dynamics in a deep, well-aerated soil, *Eur. J. Soil Sci.*, *61*, 877–887, doi:10.1111/j.1365-2389.2010.01287.x.

Marshall, T. J. (1959), The diffusion of gases through porous media, *J. Soil Sci.*, *10*(1), 79–82, doi:10.1111/j.1365-2389.1959.tb00667.x.

Massman, W. J., R. A. Sommerfeld, A. R. Mosier, K. F. Zeller, T. J. Hehn, and S. G. Rochelle (1997), A model investigation of turbulence-driven pressure-pumping effects on the rate of diffusion of CO_2, N_2O, and CH_4 through layered snowpacks, *J. Geophys. Res.*, *102*, 18,851–18,863, doi:10.1029/97JD00844.

McFarlane, K., A. Finzi, L. Nave, and J. Tang (2014), Recommendations for belowground carbon data and measurements for the AmeriFlux network. An invited white paper prepared for the AmeriFlux Network.

Millington, R. J. (1959), Gas diffusion in porous media, *Science*, *130*(3367), 100–102, doi:10.1126/science.130.3367.100-a.

Millington, R., and J. P. Quirk (1961), Permeability of porous solids, *Trans. Faraday Soc.*, *57*, 1200–1207, doi:10.1039/tf9615701200.

Moldrup, P., C. W. Kruse, D. E. Rolston, and T. Yamaguchi (1996), Modeling diffusion and reaction in soils: III. Predicting gas diffusivity from the campbell soil-water retention model, *Soil Sci.*, *161*(6).

Moldrup, P., T. Olesen, D. E. Rolston, and T. Yamaguchi (1997), Modeling diffusion and reaction in soils .7. Predicting gas and ion diffusivity in undisturbed and sieved soils, *Soil Sci.*, *162*, 632–640, doi:10.1097/00010694-199709000-00004.

Moldrup, P., T. Olesen, T. Yamaguchi, P. Schjonning, and D. E. Rolston (1999), Modeling diffusion and reaction in soils: IX. The Buckingham-Burdine-Campbell equation for gas diffusivity in undisturbed soil, *Soil Sci.*, *164*, 542–551, doi:10.1097/00010694-199908000-00002.

Moldrup, P., T. Olesen, J. Gamst, P. Schjonning, T. Yamaguchi, and D. E. Rolston (2000), Predicting the gas diffusion coefficient in repacked soil: Water-induced linear reduction model, *Soil Sci. Soc. Am. J.*, *64*, 1588–1594.

Moore, J. R., V. Gischig, M. Katterbach, and S. Loew (2011), Air circulation in deep fractures and the temperature field of an alpine rock slope, *Earth Surf. Process. Landforms*, *36*, 1985–1996, doi:10.1002/esp.2217.

Nachshon, U., M. Dragila, and N. Weisbrod (2012), From atmospheric winds to fracture ventilation: Cause and effect, *J. Geophys. Res.*, *117*, G02016, doi:10.1029/2011JG001898.

Oishi, A. C., S. Palmroth, J. R. Butnor, K. H. Johnsen, and R. Oren (2013), Agricultural and forest meteorology spatial and temporal variability of soil CO_2 efflux in three proximate temperate forest ecosystems, *Agric. For. Meteorol.*, *171-172*, 256–269, doi:10.1016/j.agrformet.2012.12.007.

Ota, M., and H. Yamazawa (2010), Forest floor CO_2 flux estimated from soil CO_2 and radon concentrations, *Atmos. Environ.*, *44*(36), 4529–4535, doi:10.1016/j.atmosenv.2010.08.031.

Penman, H. L. (1940), Gas and vapour movements in the soil: I. The diffusion of vapours through porous solids, *J. Agric. Sci.*, *30*, 437–462.

Pingintha, N., M. Y. Leclerc, J. P. Beasley Jr., G. Zhang, and C. Senthong (2010), Assessment of the soil CO_2 gradient method for soil CO_2 efflux measurements: Comparison of six models in the calculation of the relative gas diffusion coefficient, *Tellus Ser. B Chem. Phys. Meteorol.*, *62*, 47–58, doi:10.1111/j.1600-0889.2009.00445.x.

Pumpanen, J., H. Ilvesniemi, and P. Hari (2003), A process-based model for predicting soil carbon dioxide efflux and concentration, *Soil Sci. Soc. Am. J.*, *67*, 402–413.

Pumpanen, J., et al. (2004), Comparison of different chamber techniques for measuring soil CO_2 efflux, *Agric. For. Meteorol.*, *123*(3-4), 159–176, doi:10.1016/j.agrformet.2003.12.001.

Raich, J. W., and W. H. Schlesinger (1992), The global carbon dioxide flux in soil respiration and its relationship to vegetation and climate, *Tellus B*, *44*(2), 81–99.

Rains, F. A., P. C. Stoy, C. M. Welch, C. Montagne, and B. L. McGlynn (2016), A comparison of methods reveals that enhanced diffusion helps explain cold-season soil CO_2 efflux in a lodgepole pine ecosystem, *Cold Reg. Sci. Technol.*, *121*, 16–24, doi:10.1016/j.coldregions.2015.10.003.

Rey, A., L. Belelli-Marchesini, A. Were, P. Serrano-Ortiz, G. Etiope, D. Papale, F. Domingo, and E. Pegoraro (2012), Wind as a main driver of the net ecosystem carbon balance of a semiarid Mediterranean steppe in the south east of Spain, *Global Change Biol.*, *18*, 539–554, doi:10.1111/j.1365-2486.2011.02534.x.

Risk, D., C. K. Lee, C. MacIntyre, and S. C. Cary (2013), First year-round record of Antarctic Dry Valley soil CO_2 flux, *Soil Biol. Biochem.*, *66*, 193–196, doi:10.1016/j.soilbio.2013.07.006.

Rogie, J. D., D. M. Kerrick, M. L. Sorey, G. Chiodini, and D. L. Galloway (2001), Dynamics of carbon dioxide emission at Mammoth Mountain, California, *Earth Planet. Sci. Lett.*, *188*, 535–541, doi:10.1016/s0012-821x(01)00344-2.

Roland, M., S. Vicca, M. Bahn, T. Ladreiter-Knauss, M. Schmitt, and I. A. Janssens (2015), Importance of nondiffusive transport for soil CO_2 efflux in a temperate mountain grassland, *J. Geophys. Res. Biogeosci.*, *120*, 502–512, doi:10.1002/2014JG002788.

Sadeghi, A. M., D. E. Kissel, and M. L. Cabrera (1989), Estimating molecular diffusion coefficients of urea in unsaturated soil, *Soil Sci. Soc. Am. J.*, *53*, doi:10.2136/sssaj1989.03615995005300010003x.

Sanchez-Canete, E. P., and A. S. Kowalski (2014), Comment on "Using the gradient method to determine soil gas flux: A review" by M. Maier and H. Schack-Kirchner, *Agric. For. Meteorol.*, *197*, 254–255, doi:10.1016/j.agrformet.2014.07.002.

Sanchez-Canete, E. P., P. Serrano-Ortiz, A. S. Kowalski, C. Oyonarte, and F. Domingo (2011), Subterranean CO_2 ventilation and its role in the net ecosystem carbon balance of a karstic shrubland, *Geophys. Res. Lett.*, *38*, L09802, doi:10.1029/2011GL047077.

Sanchez-Canete, E. P., P. Serrano-Ortiz, F. Domingo, and A. S. Kowalski (2013a), Cave ventilation is influenced by variations in the CO_2-dependent virtual temperature, *Int. J. Speleol.*, *42*, 1–8, doi:10.5038/1827-806x.42.1.1.

Sanchez-Canete, E. P., A. S. Kowalski, P. Serrano-Ortiz, O. Perez-Priego, and F. Domingo (2013b), Deep CO_2 soil inhalation/exhalation induced by synoptic pressure changes and atmospheric tides in a carbonated semiarid steppe, *Biogeosciences*, *10*, 6591–6600, doi:10.5194/bg-10-6591-2013.

Sánchez-Cañete, E. P., R. L. Scott, J. van Haren, and G. A. Barron-Gafford (2016), Improving the accuracy of the gradient method for determining soil carbon dioxide efflux, *J. Geophys. Res. Biogeosci.*, *121*, doi:10.1002/2016JG003530.

Schack-Kirchner, H., E. Kublin, and E. E. Hildebrand (2011), Finite-element regression to estimate production profiles of greenhouse gases in soils, *Vadose Zone. J.*, *10*, 169.

Scott, R. L., G. D. Jenerette, D. L. Potts, and T. E. Huxman (2009), Effects of seasonal drought on net carbon dioxide exchange from a woody-plant-encroached semiarid grassland, *J. Geophys. Res.*, *114*, G04004, doi:10.1029/2008JG000900.

Scott, R. L., J. A. Biederman, E. P. Hamerlynck, and G. A. Barron-Gafford (2015), The carbon balance pivot point of southwestern U.S. semiarid ecosystems: Insights from the 21st century drought, *J. Geophys. Res. Biogeosci.*, *120*, 2612–2624, doi:10.1002/2015JG003181.

Seok, B., D. Helmig, M. W. Williams, D. Liptzin, K. Chowanski, and J. Hueber (2009), An automated system for continuous measurements of trace gas fluxes through snow: An evaluation of the gas diffusion method at a subalpine forest site, Niwot Ridge, Colorado, *Biogeochemistry*, *95*, 95–113, doi:10.1007/s10533-009-9302-3.

Serrano-Ortiz, P., M. Roland, S. Sanchez-Moral, I. A. Janssens, F. Domingo, Y. Godderis, and A. S. Kowalski (2010), Hidden, abiotic CO_2 flows and gaseous reservoirs in the terrestrial carbon cycle: Review and perspectives, *Agric. For. Meteorol.*, *150*, 321–329, doi:10.1016/j.agrformet.2010.01.002.

Shcherbak, I., and P. G. Robertson (2014), Determining the diffusivity of nitrous oxide in soil using in situ tracers, *Soil Sci. Soc. Am. J.*, *78*(1), 79, doi:10.2136/sssaj2013.05.0181.

Sponseller, R. A. (2007), Precipitation pulses and soil CO_2 flux in a Sonoran desert ecosystem, *Global Change Biol.*, *13*(2), 426–436, doi:10.1111/j.1365-2486.2006.01307.x.

Stoy, P. C., G. G. Katul, M. B. S. Siqueira, J.-Y. Juang, K. A. Novick, J. M. Uebelherr, and R. Oren (2006), An evaluation of models for partitioning eddy covariance-measured net ecosystem exchange into photosynthesis and respiration, *Agric. For. Meteorol.*, *141*(1), 2–18, doi:10.1016/j.agrformet.2006.09.001.

Subke, J. A., M. Reichstein, and J. D. Tenhunen (2003), Explaining temporal variation in soil CO_2 efflux in a mature spruce forest in southern Germany, *Soil Biol. Biochem.*, *35*, 1467–1483, doi:10.1016/s0038-0717(03)00241-4.

Takle, E. S., W. J. Massman, J. R. Brandle, R. A. Schmidt, X. H. Zhou, I. V. Litvina, R. Garcia, G. Doyle, and C. W. Rice (2004), Influence of high-frequency ambient pressure pumping on carbon dioxide efflux from soil, *Agric. For. Meteorol.*, *124*, 193–206, doi:10.1016/j.agrformet.2004.01.014.

Tang, J. W., D. D. Baldocchi, Y. Qi, and L. K. Xu (2003), Assessing soil CO_2 efflux using continuous measurements of CO_2 profiles in soils with small solid-state sensors, *Agric. For. Meteorol.*, *118*, 207–220, doi:10.1016/s0168-1923(03)00112-6.

Todd-Brown, K. E. O., J. T. Randerson, W. M. Post, F. M. Hoffman, C. Tarnocai, E. A. G. Schuur, and S. D. Allison (2012), Causes of variation in soil carbon predictions from CMIP5 Earth system models and comparison with observations, *Biogeosci. Discuss.*, *9*(10), 14,437–14,473, doi:10.5194/bgd-9-14437-2012.

Uchida, M., Y. Nojiri, N. Saigusa, and T. Oikawa (1997), Calculation of CO_2 flux from forest soil using [222]Rn calibrated method, *Agric. For. Meteorol.*, *87*(4), 301–311, doi:10.1016/S0168-1923(97)00001-4.

van Gorsel, E., R. Leuning, H. A. Cleugh, H. Keith, M. U. F. Kirschbaum, and T. Suni (2008), Application of an alternative method to derive reliable estimates of nighttime respiration from eddy covariance measurements in moderately complex topography, *Agric. For. Meteorol.*, *148*(6-7), 1174–1180, doi:10.1016/j.agrformet.2008.01.015.

Vargas, R., et al. (2010), Looking deeper into the soil: Biophysical controls and seasonal lags of soil CO_2 production and efflux, *Ecol. Appl.*, *20*(6), 1569–1582, doi:10.1890/09-0693.1.

Vargas, R., M. S. Carbone, M. Reichstein, and D. D. Baldocchi (2011), Frontiers and challenges in soil respiration research: From measurements to model-data integration, *Biogeochemistry*, *102*(1), 1–13, doi:10.1007/s10533-010-9462-1.

Vargas, R., S. L. Collins, M. L. Thomey, J. E. Johnson, R. F. Brown, D. O. Natvig, and M. T. Friggens (2012), Precipitation variability and fire influence the temporal dynamics of soil CO_2 efflux in an arid grassland, *Global Change Biol.*, *18*, 1401–1411, doi:10.1111/j.1365-2486.2011.02628.x.

Vaz, C. M. P., S. Jones, M. Meding, and M. Tuller (2013), Evaluation of standard calibration functions for eight electromagnetic soil moisture sensors, *Vadose Zone. J.*, *12*(2), doi:10.2136/vzj2012.0160.

Weisbrod, N., M. I. Dragila, U. Nachshon, and M. Pillersdorf (2009), Falling through the cracks: The role of fractures in Earth-atmosphere gas exchange, *Geophys. Res. Lett.*, *36*, L02401, doi:10.1029/2008GL036096.

Werner, D., P. Grathwohl, and P. Höhener (2004), Review of field methods for the determination of the tortuosity and effective gas-phase diffusivity in the vadose zone, *Vadose Zone. J.*, *3*, 1240, doi:10.2136/vzj2004.1240.

Wilhelm, E., R. Battino, and R. J. Wilcock (1977), Low-pressure solubility of gases in liquid water, *Chem. Rev.*, *77*, 219–262, doi:10.1021/cr60306a003.

Wooton, E. O. (1898), New plants from New Mexico, I–III, *Bull. Torrey Bot. Club*, *25*(8), 451–459, doi:10.2307/2477913.

Xu, X., J. L. Nieber, and S. C. Gupta (1992), Compaction effect on the gas diffusion coefficient in soils, *Soil Sci. Soc. Am. J.*, *56*, doi:10.2136/sssaj1992.03615995005600060014x.

Zhang, Q., G. G. Katul, R. Oren, E. Daly, S. Manzoni, and D. Yang (2015), The hysteresis response of soil CO_2 concentration and soil respiration to soil temperature, *J. Geophys. Res. Biogeosci.*, *120*, 1605–1618, doi:10.1002/2015JG003047.